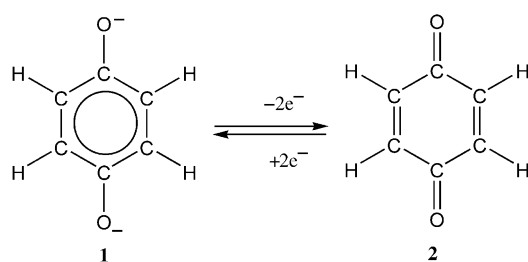


Polyhedral Boranes**Polyhedral Boranes with Exo Multiple Bonds:
Three-Dimensional Inorganic Analogues of
Quinones*****Musiri M. Balakrishnarajan and Roald Hoffmann**

Something interesting and chemically significant happens in an organic aromatic system when it is substituted with lone-pair-bearing electronegative ligands, and then oxidized. Consider the dioxobenzene dianion—benzoquinone couple **1** and **2**. There is an easy oxidation/reduction connecting these two molecules, coupled with destruction/formation of the aro-

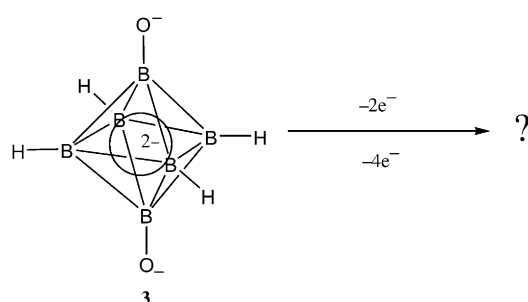
[*] Prof. Dr. R. Hoffmann, Dr. M. M. Balakrishnarajan
Department of Chemistry and Chemical Biology
Cornell University
Ithaca, NY 14853 (USA)
Fax: (+1) 607-255-5707
E-mail: rh34@cornell.edu

[**] We are grateful to the National Science Foundation (NSF) for its support of this research through its grant No. CHE-02 04841.



matic system, multiple bonding to the exocyclic substituent, and attendant strong skeletal deformation.

Polyhedral boranes are considered to be 3D aromatic systems.^[1] Could something analogous take place in polyhedral boranes on substitution by lone-pair bearing ligands? And could the effect be even stronger than in organic molecules due to the cylindrical nature of the interaction? The idea is indicated schematically in **3**.



Our motivation for thinking about exohedral multiple bonds on a polyhedral skeleton was triggered by the observation of conjugative effects across ten and twelve vertex *bi-para*-substituted boranes and carboranes with phenyl, pyridinyl and dinitrogen substituents.^[2–5] As electronic communication across the polyhedral skeleton essentially involves some π character in the bond connecting these substituents to the polyhedral skeleton, we wondered whether such partial π bonding could be maximized for a suitable electron count. Herein, we explore the relatively simple octahedral and pentagonal bipyramidal borane skeletons with exo multiple bonds. All the systems considered here are studied by using hybrid DFT calculations (B3LYP-6-311 + G**),^[6] a fragment molecular-orbital (MO) analysis is performed by using extended Hückel calculations.^[7] The extension of these to higher boranes and their energetics will be reported elsewhere.

We selected the disubstituted O, NH and S derivatives for the study. The substitution of these groups at the *para* positions of the *closo*-borane $B_6H_6^{2-}$ will result in $B_6H_4X_2^{4-}$ ($X = O, NH, S$), classical Wade systems. In fact, we had to carry out calculations on the di and tetraprotonated forms of these, as the parent tetraanion calculations failed to converge in the geometry optimization. To move toward multiple bonding, we removed one or two electron pairs from $B_6H_4X_2^{4-}$, leading to $B_6H_4X_2^{2-}$ or $B_6H_4X_2$, respectively. DFT calculations show that all of these dianions and neutrals are minima (Table 1). The various B–B distances calculated are

Table 1: The point group, and Wiberg Bond Orders (WBO) for B–X bonds, computed at B3LYP6-311 + G** level of theory for various $B_6H_4X_2^{2-}$, $B_7H_5X_2^{2-}$ and $B_8X_6^{2-}$ systems. The HOMO–LUMO gap (Gap) is obtained from eH calculations using the ab initio optimized geometry; LUMO = lowest-unoccupied molecular orbital.

No	Molecule	Symmetry	Gap(eV)	WBO
1	$B_6H_4O_2^{2-}$	D_{2h}	0.68	1.39
2	$B_6H_4(NH)_2^{2-}$	C_{2h}	0.66	1.38
3	$B_6H_4S_2^{2-}$	D_{2h}	0.53	1.52
4	$B_6H_4O_2$	D_{4h}	0.71	1.72
5	$B_6H_4(NH)_2$	D_{4h}	1.38	1.78
6	$B_6H_4S_2$	D_{4h}	1.01	1.91
7	$B_7H_5O_2^{2-}$	D_{5h}	0.28	1.38
8	$B_7H_5(NH)_2^{2-}$	C_1	0.26	1.34
9	$B_7H_5S_2^{2-}$	D_{5h}	0.19	1.47
10	$B_8O_6^{2-}$	O_h	3.35	1.57
11	$B_8S_6^{2-}$	O_h	2.35	1.81

given in Figure 1. In the dianions, there is pronounced bond alternation in the “belt” of the polyhedron, to which we will return later.

The exopolyhedral B–X bond lengths decrease steadily and dramatically when the systems are oxidized (as in quinones). For example, the B–O bond length 1.574 Å in $B_6H_4(OH)_2$ (tetraprotonated $B_6H_4O_2^{4-}$) decreases to 1.296 Å in $B_6H_4O_2^{2-}$ and further decreased to 1.227 Å in $B_6H_4O_2$.^[8] In all the oxidized systems, the bonds that connect the substituted boron atoms to the central B_4H_4 ring are also elongated compared to the unoxidized systems. This short–long–short alternation is parallel to what happens in quinones. In addition, the B–B bonds of the belt B_4H_4 ring fragment in the $B_6H_4X_2^{2-}$ series show pronounced bond alternation, much like cyclobutadiene. As we shall see, the relationship is not an accident.

A similar substitution sequence in the *closo*- B_7 skeleton gives $B_7H_5O_2^{2-}$, $B_7H_5(NH)_2^{2-}$ and $B_7H_5S_2^{2-}$ ions—all of them characterized as stationary points at the same level of theory. In this case, however, further oxidation to the neutral species $B_7H_5X_2$ breaks the *closo*- B_7 the skeleton for all the substituents considered here. In the *closo*- B_7 skeletons of $B_7H_5X_2^{2-}$, bonds are elongated along the major symmetry axis and they also exhibit bond alternation in their belts (Figure 2); the B–B bond lengths of the central B_5H_5 ring in the pattern longer–short–long–short–longer.

To understand the origin of the fascinating bond alternation in $B_6H_4X_2^{2-}$ and $B_7H_5X_2^{2-}$, we studied the nature of π -orbital interactions between the borane skeleton and the exo substituent by extended Hückel calculations. Figure 3 shows the interaction of frontier orbitals of B_6H_4 and B_7H_5 fragments with $(O)_2$ π orbitals, building up $B_6H_4O_2^{4-}$ (D_{4h}) and $B_7H_5O_2^{4-}$, respectively.^[9] All the levels shown in the figure are filled in the tetraanions. The triply degenerate highest-occupied molecular orbital (HOMO; t_{1g}) of the *closo*- $B_6H_6^{2-}$ borane^[10] (which arises from the in-phase combination of tangential p orbitals of boron) splits into $b_{2g} + e_g$ due to the substitution by oxygen atoms (upper left of Figure 3). While b_{2g} by symmetry remains unaffected by oxygen π orbitals, the e_g set interacts with the out-of-phase combination (π_g) of $(O)_2$ to give a pair of bonding and antibonding MOs, the latter forming the HOMO of $B_6H_4O_2^{4-}$.

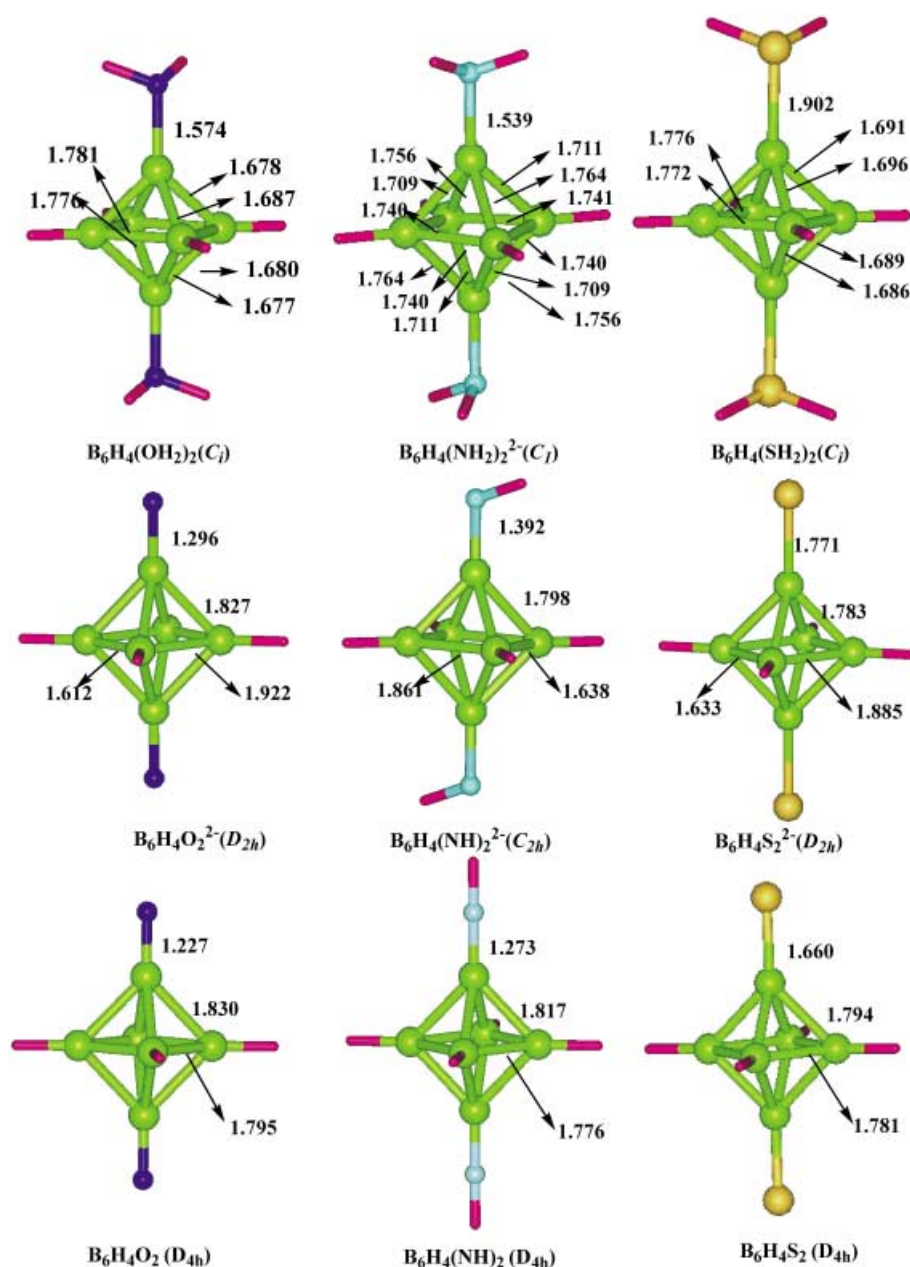


Figure 1. Closo-B₆ systems having exo multiple bonds, with their bond lengths (in Å) calculated at B3LYP6-311+G** level of theory.

Removal of an electron pair from the “Wadian” B₆H₄O₂⁴⁻ to form B₆H₄O₂²⁻ generates a classical Jahn–Teller situation; a distortion ensues, thus stabilizing one of the degenerate MOs. Figure 4 shows one representation of the degenerate pair of orbitals on the left, another combination on the right. Focusing on the equatorial B₄ ring in these orbitals, we see the direct parallel to the orbitals of cyclobutadiene. The outcome of the Jahn–Teller distortion, as in cyclobutadiene, is pronounced bond alternation within the square B₄H₄ ring.

The B₇H₅ fragment interacts with (O)₂ in a similar way. Though the π -type orbitals of the B₇H₅ fragment are slightly below the HOMO in B₇H₇²⁻, they do mix strongly with the out-of-phase combination of the π orbitals of the exopolyhedral (O)₂ fragment, the antibonding combination forming the

HOMO of B₇H₅O₂⁴⁻. Again, removal of two electrons will generate a Jahn–Teller situation, resulting eventually in two of the bonds in B₇H₅X₂ systems being shorter than the other three.

In B₆H₄X₂, all four electrons are removed from the doubly degenerate HOMO, leading to a return to D_{4h} symmetry. Successive oxidation removes electrons from MOs that are antibonding between the borane skeleton and the substituents, and bonding within the polyhedron. This is reflected in the shortened B–X bond lengths, indicative of multiple bonding, and in bond expansion in the polyhedron (see Figure 1).

To assess the magnitude of multiple bonding, we calculated the Wiberg bond order (WBO)^[11] by using NBO routines^[12] in Gaussian 98 (Table 1). The WBO values of the B–X bond in the parent protonated forms are 0.56, 0.89 and 0.83 for –OH, –SH₂ and –NH₂ groups respectively. On oxidation, the WBO values are increased to more than one for B₆H₄X₂²⁻ and further increased to more than 1.5 for the neutral B₆H₄X₂ series. This can be compared with the organic analogues C₆H₄O₂²⁻ and C₆H₄(OH)₂, whose WBO values are 1.26 and 1.75, respectively, at the same level of theory.

Though the bond multiplicity of these B–X bonds is not provided by the B–X bond order values, the trends are indicative. There is clearly exopolyhedral multiple bonding.^[13] In the case of neutral B₆H₄(NH)₂, the B–N–H bond angle is exactly 180°, which is also indi-

cative of a cylindrical B≡N type interaction. The HOMO–LUMO gap, which is a fair measure of reactivity,^[14] suggests that the dianionic systems are more reactive than the neutral systems. We believe the sum of the theoretical evidence supports the assertion that these systems are the natural 3D analogues of benzoquinone in polyhedral systems.

It is also possible to restore the octahedral geometry of the B₆ skeleton in B₆H₆²⁻ with six multiply bonded exohedral substituents. DFT calculations on B₆O₆²⁻ (O_h) and B₆S₆²⁻ (O_h) show that they are indeed minima on their potential energy surface (Figure 5).

The two-electron requirement of these systems can be explained by analyzing the nature of the π -type interactions. The occupied levels of a classical Wade framework set for the

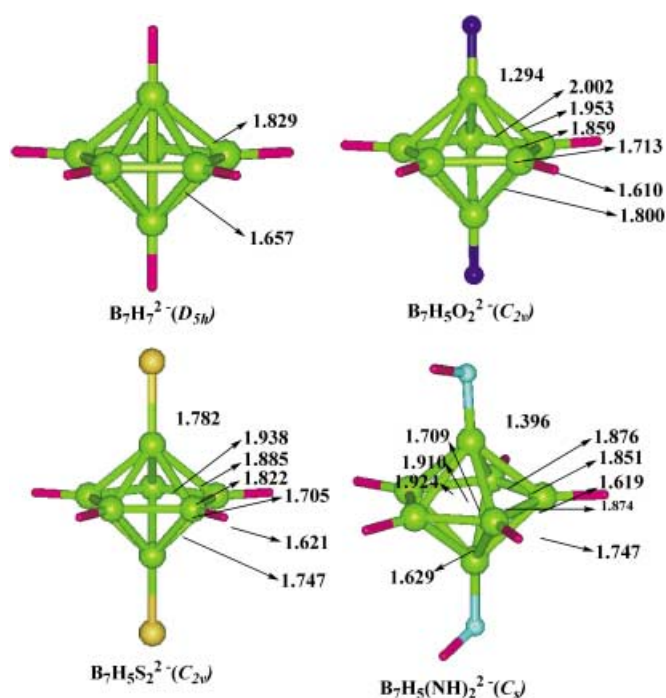


Figure 2. Closo-B₇ systems having exo multiple bonds, with bond lengths (in Å) as calculated at B3LYP6-311 + G** level of theory. B₇H₇²⁻ is included for calibration.

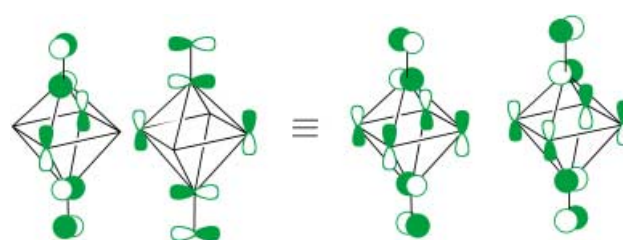


Figure 4. Two different ways of representing the e_g HOMO of B₆H₄X₂⁴⁻, occupied only by two electrons in the dianions.

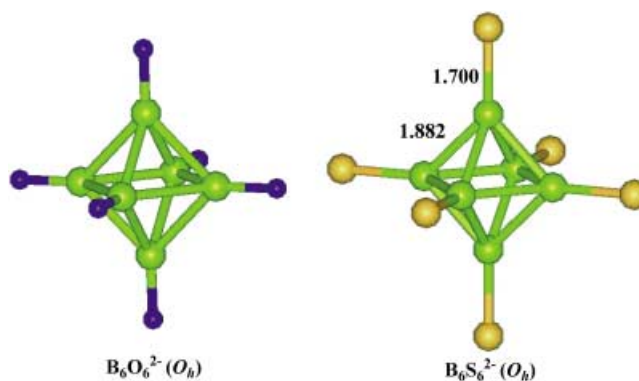


Figure 5. Closo-B₆X₆²⁻ systems having exo multiple bonds, with bond lengths (in Å) as calculated at B3LYP6-311 + G** level of theory.

B₆ cluster include two triply degenerate orbitals of tangential character; set up for interaction with external π systems; a purely tangential t_{2g}, and a t_{1u} that has a mixture of tangential and radial character. These are shown at left of Figure 6. The

12 π-type orbitals of the six external O substituents in a hypothetical B₆O₆⁸⁻ (B₆H₆²⁻ to B(OH)₆²⁻ to B₆O₈⁸⁻ + 6H⁺) transform as t_{2g} + t_{1u} + t_{2u} + t_{1g}. Of these t_{2u} and t_{1g} do not interact much with the polyhedron MOs. Cluster t_{2g} and t_{1u}

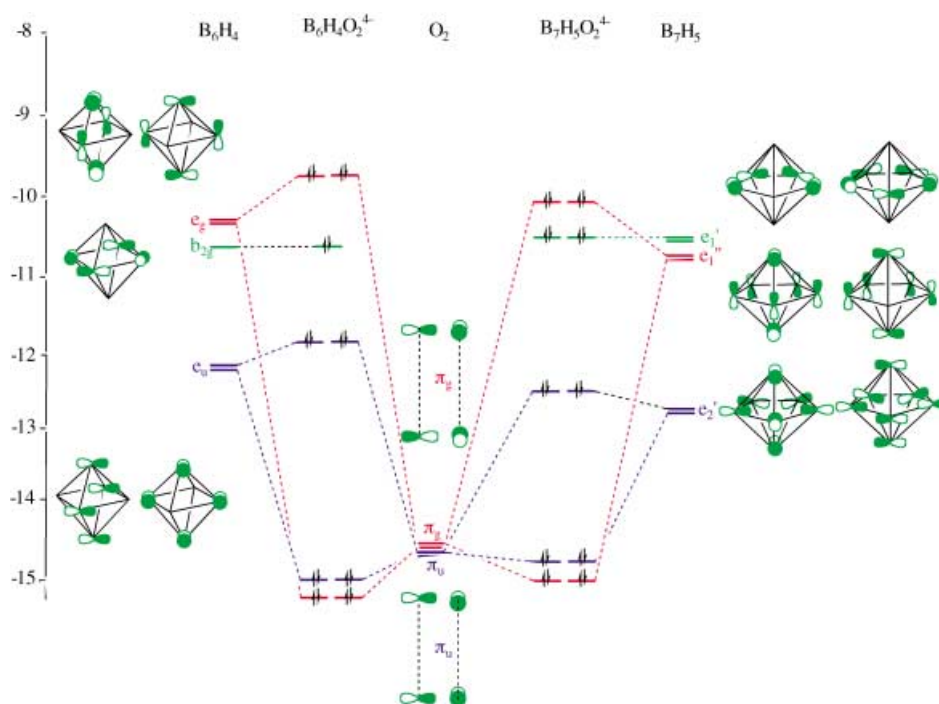


Figure 3. The interaction of the B₆H₄ (D_{4h}) and B₇H₅ (D_{5h}) fragments with two oxygen atoms (D_{∞h}), leading to the bonding MOs of closo-B₆H₄O₂⁴⁻ and closo-B₇H₅O₂⁴⁻.

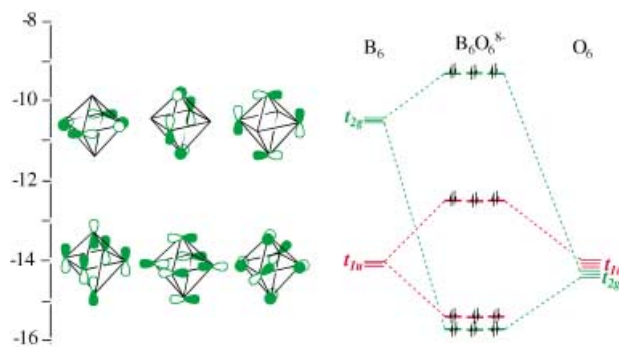


Figure 6. The interaction of $B_6(O_6)$ fragment with six oxygen atoms (O_6), resulting in the bonding MOs of $closo-B_6O_6^{2-}$.

MOs form antibonding combinations with the corresponding symmetry oxygen lone pair combinations, as illustrated in Figure 6. A good HOMO-LUMO gap results if the t_{2g} antibonding combination is unfilled, which implies a six electron oxidation of $B_6O_6^{8-}$ to $B_6O_6^{2-}$. The next closed shell structure is at $B_6O_6^{4+}$, which is not realistic. Since these MOs are antibonding between the two fragments, the removal of electrons results in π bonding.

These hypothetical polyhedral ions may be viewed as electronically equivalent to the oxocarbon dianions such as $C_3O_3^{2-}$, $C_4O_4^{2-}$, $C_5O_5^{2-}$ and $C_6O_6^{2-}$.^[15] The boron systems show substantial HOMO-LUMO gaps (Table 1). Given all the useful chemistry of quinones and oxocarbon dianions, we believe that interesting structures and reactivity will be found in these 3D analogues.

Received: May 6, 2003 [Z51821]

Keywords: ab initio calculations · aromaticity · boranes · Jahn-Teller distortion · multiple bonds

Yang, R. G. Parr, *Phys. Rev. B* **1988**, 37, 785; e) S. H. Vosko, L. Wilk, M. Nusair, *Can. J. Phys.* **1980**, 58, 1200; f) P. J. Stephens, F. J. Delvin, C. F. Chabalowski, M. J. Frisch, *J. Phys. Chem.* **1994**, 98, 11 623.

[7] a) R. Hoffmann, W. N. Lipscomb, *J. Chem. Phys.* **1962**, 36, 2179; b) R. Hoffmann, *J. Chem. Phys.* **1963**, 39, 1397.

[8] This can be compared with the polyhedral B-X bond lengths in experimentally known compounds: B-O = 1.480 ($B_{12}H_{11}OH^{2-}$), B-N = 1.521 ($B_{12}H_{11}[NH_3]^{-1}$), B-S = 1.862 ($B_{12}H_{11}SH^{2-}$). I. B. Sivaev, V. I. Bregadze, S. Sjöberg, *Collect. Czech. Chem. Commun.* **2002**, 67, 679.

[9] These orbital patterns are also seen in the DFT calculations.

[10] a) T. A. Albright, J. K. Burdett, M. Whangbo, *Orbital Interactions in Chemistry*, Wiley, New York, **1985**, chap. 22; b) M. A. Fox, K. Wade in *The Borane, Carborane, Carbocation continuum* (Ed.: J. Casanova), Wiley, New York, **1998**, p. 7.

[11] E. D. Glendening, A. E. Reed, J. E. Carpenter, F. Weinhold, NBO version 3.1, University of Wisconsin, WI, 1995.

[12] K. B. Wiberg, *Tetrahedron* **1968**, 24, 1083.

[13] In the oxidized derivatives of $B_{12}(OR)_{12}^{2-}$ there is already some indication of exohedral multiple bonding and polyhedral deformation: T. Peymann, C. B. Knobler, S. I. Khan, M. F. Hawthorne, *Angew. Chem.* **2001**, 113, 1713; *Angew. Chem. Int. Ed.* **2001**, 40, 1664; see also M. L. McKee, *Inorg. Chem.* **2002**, 41, 1299.

[14] For comparison, the HOMO-LUMO gaps in $B_6H_6^{2-}$, $B_7H_7^{2-}$ and $B_{12}H_{12}^{2-}$ are 6.55 eV, 6.55 eV and 7.25 respectively.

[15] G. Seitz, P. Imming, *Chem. Rev.* **1992**, 92, 1227.

- [1] J. I. Aihara, *J. Am. Chem. Soc.* **1978**, 100, 3339; b) I. Gutman, M. Milun, N. Trinajstić, *J. Am. Chem. Soc.* **1977**, 99, 1692.
- [2] P. Kaszynski, A. G. Doughlass, *J. Organomet. Chem.*, **1999**, 581, 28.
- [3] W. H. Knoch, *J. Am. Chem. Soc.* **1966**, 88, 935.
- [4] P. Kaszynski, J. Huang, G. S. Jenkins, K. A. Bairamov, D. Lipiak, *Mol. Cryst. Liq. Cryst.* **1995**, 260, 315.
- [5] M. A. Fox, J. A. H. Macbride, R. J. Peace, K. Wade, *J. Chem. Soc. Dalton Trans.* **1998**, 401.
- [6] a) Gaussian 98 (Revision A.7), M. J. Frisch, G. W. Trucks, H. B. Schlegel, G. E. Scuseria, M. A. Robb, J. R. Cheeseman, V. G. Zakrzewski, J. A. Montgomery, R. E. Stratmann, J. C. Burant, S. Dapprich, J. M. Millam, A. D. Daniels, K. N. Kudin, M. C. Strain, O. Farkas, J. Tomasi, V. Barone, M. Cossi, R. Cammi, B. Mennucci, C. Pomelli, C. Adamo, S. Clifford, J. Ochterski, G. A. Petersson, P. Y. Ayala, Q. Cui, K. Morokuma, D. K. Malick, A. D. Rabuck, K. Raghavachari, J. B. Foresman, J. Cioslowski, J. V. Ortiz, B. B. Stefanov, G. Liu, A. Liashenko, P. Piskorz, I. Komaromi, R. Gomperts, R. L. Martin, D. J. Fox, T. Keith, M. A. Al-Laham, C. Y. Peng, A. Nanayakkara, C. Gonzalez, M. Challacombe, P. M. W. Gill, B. G. Johnson, W. Chen, M. W. Wong, J. L. Andres, M. Head-Gordon, E. S. Replogle, J. A. Pople, Gaussian, Inc., Pittsburgh, PA, **1998**; b) B3LYP is Becke's three parameter hybrid method with LYP correlation functional: c) A. D. Becke, *J. Chem. Phys.* **1993**, 98, 5648; d) C. Lee, W.